Astronomy & Astrophysics

Chromospheric activity on the RS Canum Venaticorum binary SZ Piscium

L.-Y. Zhang[1,2] and S.-H. Gu[1]

[1] National Astronomical Observatories/Yunnan Observatory, Joint laboratory for Optical Astronomy, Chinese Academy of Sciences, Kunming 650011, PR China
e-mail: liy_zhang@hotmail.com

[2] Graduate School of Chinese Academy of Sciences, Beijing 100039, PR China

ABSTRACT

Aims. We present the new high-resolution echelle spectra of SZ Psc, obtained in Nov. 2004 and Sep.−Dec. 2006, and study its chromospheric activity.

Methods. By means of the spectral subtraction technique, we analyze our spectroscopic observations including several optical chromospheric activity indicators (the He I D_3, Na I D_1, D_2, H_α, and Ca II infrared triplet lines).

Results. All indicators show that the chromospheric activity of the system is associated with the cooler component. We find that the values of EW_{8542}/EW_{8498} are in the range 1−3, which indicates optically thick emission in plage-like regions. The 2006 data suggest the presence of active longitude phenomena. For the Ca II 8542 and 8662 and the H_α lines, it seems that the excess emission is stronger near the two quadratures of system. This may be anti-correlated with the behavior of the Na I D_1 line. The absorption features are detected in the subtracted H_α lines, which could be explained by prominence-like extended material seen on the stellar disk or by mass transfer from the cooler component to the hotter one.

Key words. stars: binaries: eclipsing – stars: binaries: spectroscopic – stars: chromospheres – stars: activity – stars: late-type – stars: individual

1. Introduction

SZ Psc (HD 219113, $P_{orb} = 3^d97$) is a partially eclipsing and double-lined spectroscopic binary consisting of F8V-IV hotter and K1IV cooler components (Jakate et al. 1976). Hall (1976) defined it as a typical member of RS CVn binaries, which are characterized by strong magnetic activity that presents as photospheric spots, chromospheric emission, transition region emission, coronal X-ray radiation, and flare events.

The first variability of the lightcurve of SZ Psc was found by Jensch (1934). Since then, the light-curve variations have been analyzed by many authors (Jakate et al. 1976; Eaton 1977; Catalano et al. 1978; Eaton et al. 1982; Tunca 1984; Doyle et al. 1994a; Antonopoulou et al. 1995; Lanza et al. 2001; Kang et al. 2003; Eaton & Henry 2007). For the distortion wave on the lightcurves of SZ Psc, this has been explained by the starspot model (Eaton & Hall 1979; Lanza et al. 2001; Kang et al. 2003; Eaton & Henry 2007).

The spectroscopic observations have been carried out by many groups (Jakate et al. 1976; Bopp & Talcott 1978; Weiler 1978; Bopp 1981; Ramsey & Nations 1981; Huenemoerder & Ramsey 1984; Fernández-Figueroa et al. 1986; Popper 1988; Fernández-Figueroa et al. 1994; Frasca & Catalano 1994; Montes et al. 1995; Eaton & Henry 2007). Jakate et al. (1976) and Popper (1988) derived the spectroscopic orbital elements on the basis of the radial velocity curves, and they also found strong chromospheric emission in the Ca II H & K lines from the cooler component. A flare-like phenomenon was detected in the Ca II H & K lines by Fernández-Figueroa et al. (1986). Recently, Eaton & Henry (2007) have revised the orbital elements of the system,

but so far there has been no spectroscopic study of the Ca II IRT lines for SZ Psc.

SZ Psc is very active, because of its extremely variable H_α profiles. In 1978, Weiler (1978) found that SZ Psc only exhibited significant variation in its H_α emission lines near orbital phase 0.8. Moreover, Bopp & Talcott (1978) confirmed this result and found H_α emission only in the phase range 0.6−0.8. However, Ramsey & Nations (1981) found H_α emission is in the phase range 0−0.4 and interpreted the H_α behavior as a flare event that locally injects material into a transient disk or shell structure around the K1 IV star. Afterward, Bopp (1981) discussed an unusual H_α profile, particularly its large width and double-peaked appearance. Beyond that, Huenemoerder & Ramsey (1984) found that SZ Psc was highly active with the emission from a cooler component and that it had undergone a large H_α outburst during and after which the profiles were suggestive of a circumstellar origin. The extremely variable H_α profiles suggest there are two active longitudes. Recently, Eaton & Henry (2007) have found that H_α emission seems independent of the orbital phase on average, but it can increase markedly within a few orbital cycles.

Up to now, the spectral subtraction technique has been used widely for chromospherically active binary systems in several lines: Ca II H & K, Mg I b, He I D_3, Na I D_1, D_2, H_α, H_β, Ca II IRT (Gunn & Doyle 1997; Gunn et al. 1997; Lázaro & Arévalo 1997; Montes et al. 1997; Arévalo & Lázaro 1999; Frasca et al. 2000; Montes et al. 2000; Shan et al. 2006; Gálvez et al. 2007, etc.). The technique was described in detail for obtaining the chromospheric contribution by Barden (1984) and Montes et al. (1995). Also, it was discussed and applied in the
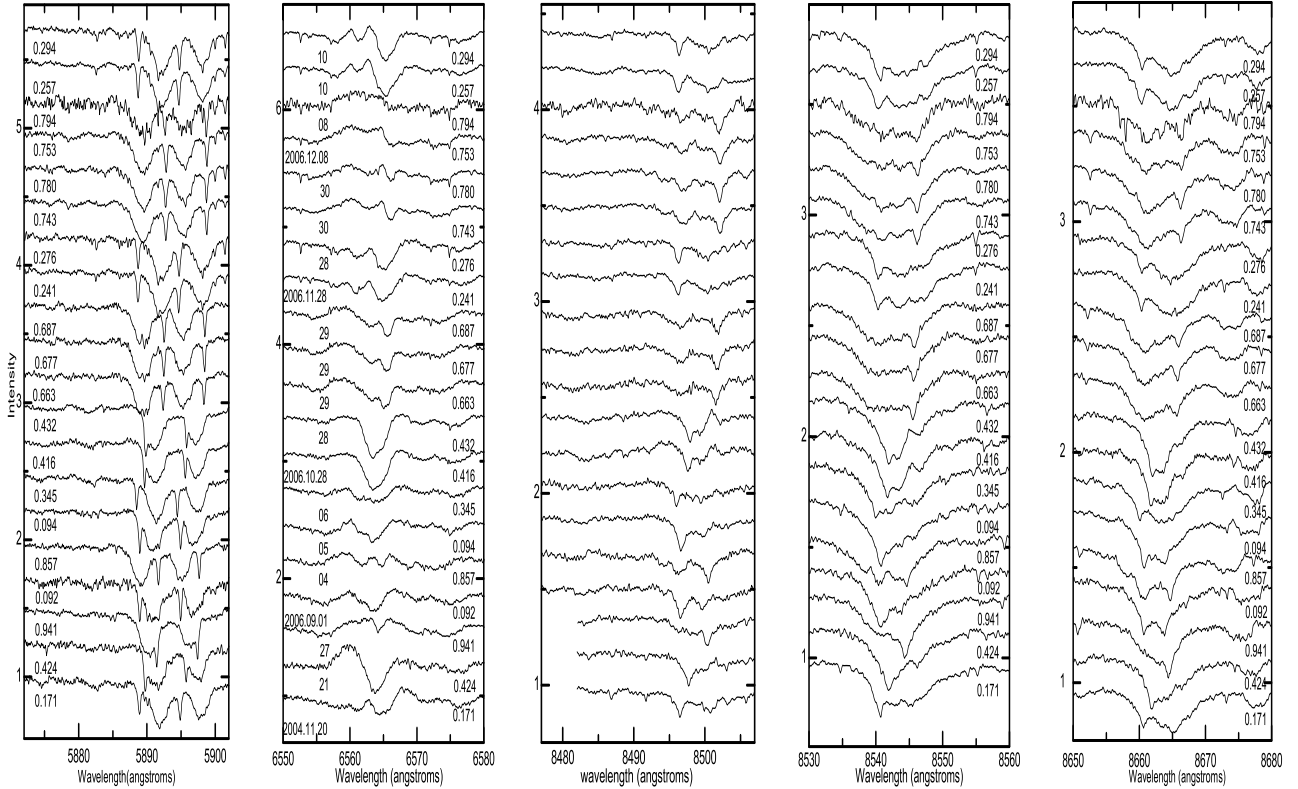
Fig. 1. The He I D$_3$, Na I D$_1$, D$_2$, H$_\alpha$, and Ca II IRT line profiles of SZ Psc.

search for prominence-like events (Gunn & Doyle 1997; Gunn et al. 1997).

In this paper, new spectroscopic observations of SZ Psc are analyzed using the spectral subtraction technique. Some new results are derived for the chromospherically active activity of SZ Psc.

2. Observation

The new spectroscopic observations of SZ Psc were carried out with the 2.16 m telescope at the Xinglong station of the National Astronomical Observatories, China, in five observing runs: Nov. 20−27, 2004, Sep. 1−6, 2006, Oct. 28−29, 2006, Nov. 28−30, 2006, and Dec. 8−10, 2006. The Coudé echelle spectrograph with a spectral resolution about 37 000 and a 1024 × 1024 pixel Tektronix CCD detector were used during our observations. The reciprocal dispersions are 0.079 Å/pixel for the He I D$_3$, Na I D$_1$, D$_2$ spectral region, 0.089 Å/pixel for the H$_\alpha$ spectral region, 0.113 Å/pixel for the Ca II 8498 spectral region, 0.115 Å/pixel for the Ca II 8542 spectral region, and 0.117 Å/pixel for the Ca II 8662 spectral region. Correspondingly, the spectral resolution determined as the FWHM of the arc comparison lines is 0.150, 0.160, 0.207, 0.218, and 0.221 Å, respectively.

The spectra were reduced using the IRAF package. The standard procedures were used, which include image trimming, bias subtraction, flat-field division, background subtraction, cosmic ray removal, and spectrum extraction. The wavelength calibration was obtained by taking the spectra of a Th-Ar lamp. Finally, the spectra were normalized by a polynomial fit to the observed continuum. The normalized spectral profiles are displayed in Fig. 1. During our observations, the signal-to-noise ratio (S/N)

Table 1. The observational log of SZ Psc.

Date	HJD	Phase	Exp. time	S/N				
	2 450 000+		(s)	Na I	H$_\alpha$	λ8498	λ8542	λ8662
2004.11.20	3330.1056	0.171	2400	122	169	146	172	158
2004.11.21	3331.1074	0.424	2400	72	102	104	121	111
2004.11.27	3337.1254	0.941	2400	92	122	105	119	109
2006.09.01	3980.1606	0.092	3600	60	89	114	125	119
2006.09.04	3983.1945	0.857	4200	107	137	136	146	137
2006.09.05	3984.1343	0.094	3600	121	161	159	173	162
2006.09.06	3985.1275	0.345	3600	148	197	191	210	195
2006.10.28	4036.9631	0.416	3600	159	208	190	211	198
2006.10.28	4037.0292	0.432	3600	174	231	216	241	225
2006.10.29	4037.9423	0.663	3600	105	137	130	141	131
2006.10.29	4037.9973	0.677	3600	101	134	130	141	131
2006.10.29	4038.0403	0.687	3600	105	139	138	149	141
2006.11.28	4067.9936	0.241	3000	105	136	135	150	140
2006.11.28	4068.1349	0.276	2400	76	107	110	122	114
2006.11.30	4069.9877	0.743	3000	110	142	135	148	138
2006.11.30	4070.1315	0.780	3000	92	136	133	152	140
2006.12.08	4077.9560	0.753	3600	82	108	106	118	110
2006.12.08	4078.1179	0.794	3600	37	52	55	61	58
2006.12.10	4079.9561	0.257	3600	123	162	157	173	161
2006.12.10	4080.1039	0.294	3600	92	136	136	152	141

varied in quality, and in some instances it suffered from poor seeing and intermittent clouds. For most of the observations, the S/N is more than 100. The observing log is listed in Table 1, which includes the observing date, the Heliocentric Julian Date of observation (HJD), orbital phase, exposure time, and the S/N. The orbital phases were calculated using the revised ephemeris derived by Eaton & Henry (2007).

On some nights of our observing seasons when the telluric lines were heavy, two rapidly rotating early-type stars,
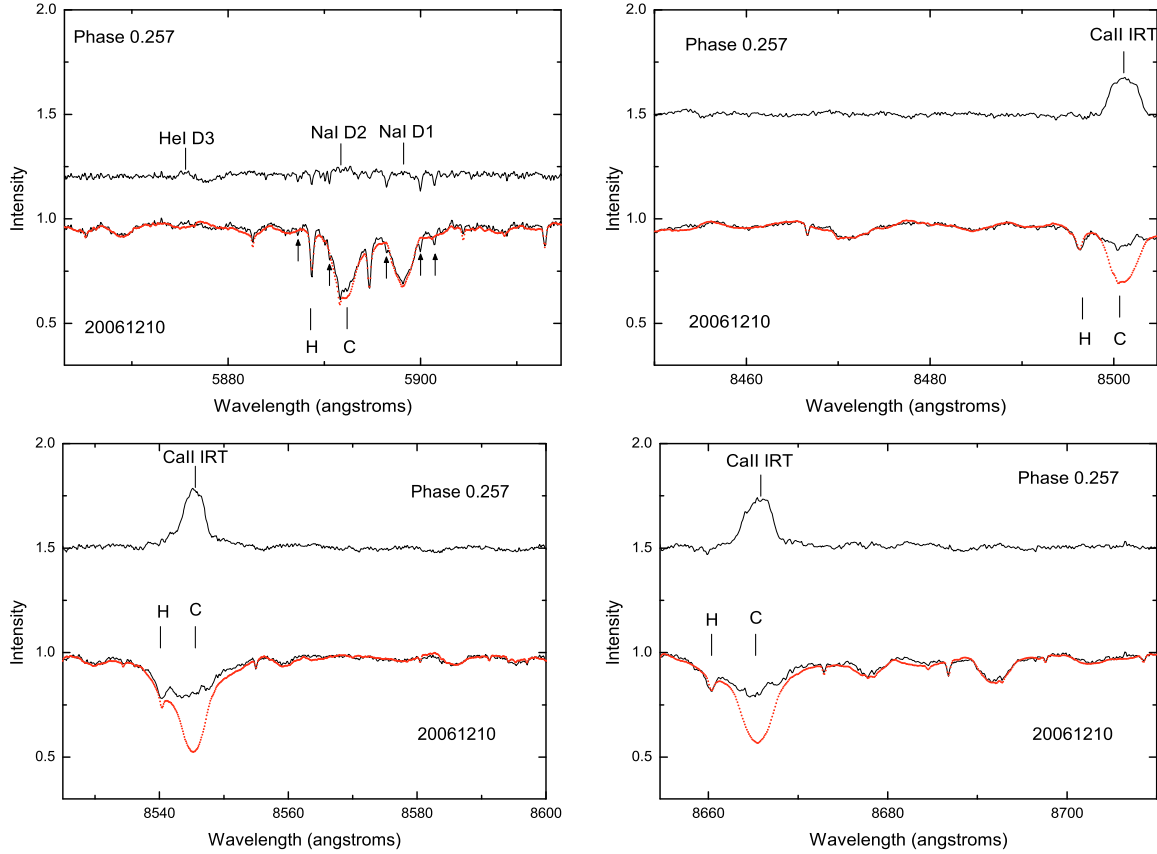
Fig. 2. Samples of the observed, synthesized, and subtracted spectra for the He I D$_3$, Na I D$_1$, D$_2$, and Ca II IRT lines. The dotted lines represent the synthesized spectra and the upper spectra are the subtracted spectra. Vertical arrows mark the telluric lines that appeared in the spectral region.

HR 7894 (B5IV, $v \sin i$ = 330 km s^{-1}) and HR 989 (B5V, $v \sin i$ = 298 km s^{-1}), were observed. Their observed spectra were fitted using the high-order spline3 function to derive the telluric line templates. For the spectra of HR 989, interstellar Na I lines were present and removed. The telluric lines in the spectra of SZ Psc were removed by means of these templates obtained on the same nights. The examples of this procedure in different spectral regions were given by Gu et al. (2002).

3. Spectral analysis

The normalized spectra of SZ Psc are analyzed using the spectral subtraction technique. In this method, the synthesized spectra is constructed from artificially rotationally broadened, radial-velocity shifted, and weighted spectra of two inactive stars with the same spectral type and luminosity class as the two components of the active system. For our situation, the synthesized spectrum is constructed by means of the program STARMOD (Barden 1985). We observed several stars with spectral types and luminosity classes similar to those of the individual components of SZ Psc. By comparison, we find that two inactive stars HR 7948 (K1IV) and HR 6669 (F8V) are much better templates for SZ Psc. Thus, we chose them as template stars to construct synthesized spectra for all spectral data of SZ Psc. For the hotter component, Strassmeier et al. (1993) gave F8 IV for the spectral type. However, we find that HR 6669 is a better template for the hotter component. Moreover, HR 6669 does have the advantage of being an extremely inactive star (Wright et al. 2004), and Gray et al. (2001) gave F8 V for its spectral type, so the spectral type of the hotter component should be F8V.

In the course of the analysis, the $v \sin i$ values (0/78 km s^{-1}) of the components of SZ Psc were used, which are determined from the spectra spanning the wavelength ranges 6389−6477 Å and 6615−6706 Å with many photospheric lines. These values are close to 80 km s^{-1} for the cooler component and less than 5 km s^{-1} for the hotter component, as published by Eaton & Henry (2007). The intensity weight for each of the two components is obtained from high-quality spectra around phases 0.25 and 0.75 where the two components are separated well. Consequently, the adopted intensity weight ratios are 0.25/0.75 for He I D$_3$ and Na I D$_1$, D$_2$ spectral region, 0.20/0.80 for H$_\alpha$ spectral region, 0.18/0.82 for the Ca II 8498 spectral region, 0.175/0.825 for the Ca II 8542 spectral region, and 0.17/0.83 for the Ca II 8662 spectral region.

Samples of the synthesized and subtracted spectra (the observed spectra minus the synthesized one) obtained in the He I D$_3$, Na I D$_1$, D$_2$, and Ca II IRT line regions are displayed in Fig. 2. Since the H$_\alpha$ features are bizarre, some samples are displayed in Fig. 3. For each sample, we plot the observed (lower solid line), the synthesized (dashed line), and the subtracted spectra (upper solid line), which is offset for better display. In these figures, "H" and "C" represent the hotter and cooler components, respectively.

4. Chromospheric activity indicators

The new spectroscopic observations allow us to simultaneously analyze the behavior of the different chromospheric activity indicators formed at different atmospheric heights.
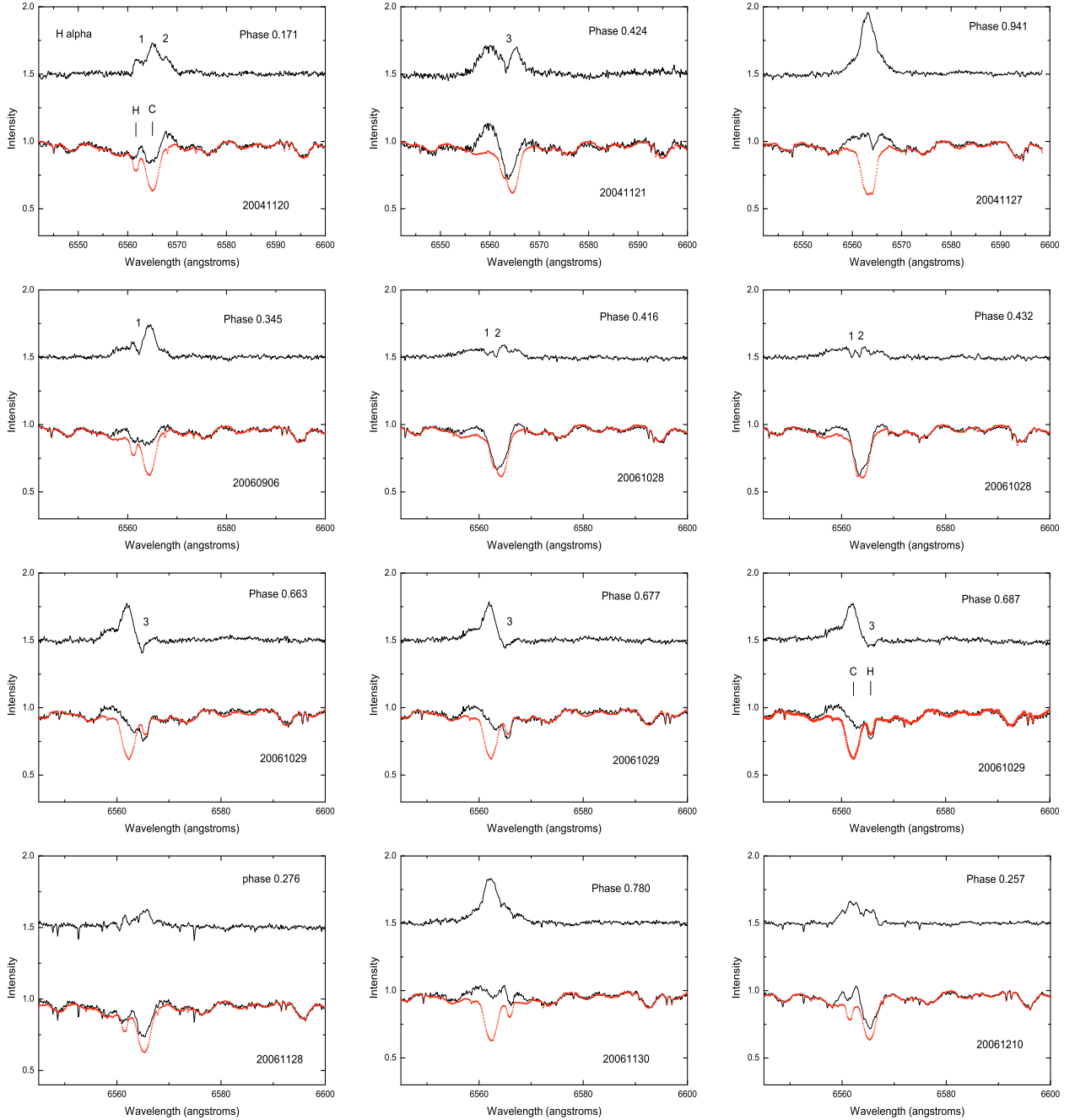
Fig. 3. Samples of the profiles of the H_α lines. The dotted lines represent the synthesized spectra. The upper spectra are the subtracted spectra. The number indicates that the absorption events appeared in the excess emission profiles.

The equivalent widths (*EW*s) of the excess emissions were measured using the IRAF SPLOT task. When the profiles of two components are easily separated, the *EW*s were evaluated on the subtracted spectra by integrating over the emission profile. In addition, we measured the *EW*s using the Gaussian fit (For asymmetric profiles, we used several Gaussian profiles to fit), If the profiles are blended, we measured the *EW*s using several Gaussian fits. For comparison, we also measured the *EW*s with the Lorenzian fit. The errors of the *EW*s were estimated by using the difference between the results of these different methods. The net *EW*s of the excess emissions are listed in Table 2.

Because of nearly a 4 integral-day period for SZ Psc, it was very difficult to observe effectively, and the phase coverage interval of observation was short per night at a single site, so we only had a few spectra per night. To discuss the rotational modulation of chromospheric activity, we used all of the 2006 data because we only have 3 to 4 data points per rotation in different epochs.

4.1. The Na I D_1, D_2, and He I D_3 lines

The Na I D_1, D_2 lines are formed in the upper photosphere and lower chromosphere. The filled-in absorption of the core of the Na I D_1, D_2 lines could be used as chromospheric activity indicators (Andretta et al. 1997; Monte et al. 1997).

The Na I D lines are characterized by deep absorption (see Fig. 1). The core of the lines does not show any reversal. The application of the spectral subtraction technique reveals that the

Table 2. The measurements for the excess emissions of the Na I D_1, D_2, H_α, and Ca II IRT lines.

Phase	EW_{NaID_1}(Å)	EW_{NaID_2}(Å)	EW_{H_α}(Å)	$EW_{CaII\ 8498}$(Å)	$EW_{CaII\ 8542}$(Å)	$EW_{CaII\ 8662}$(Å)	EW_{8542}/EW_{8498}
0.171	0.067 ± 0.006	–	1.053 ± 0.114	0.798 ± 0.002	1.224 ± 0.025	0.932 ± 0.016	1.534 ± 0.027
0.424	0.149 ± 0.020	0.066 ± 0.014	1.503 ± 0.020	0.796 ± 0.025	1.361 ± 0.036	0.986 ± 0.007	1.710 ± 0.008
0.941	0.080 ± 0.008	0.049 ± 0.003	1.908 ± 0.004	0.827 ± 0.002	1.425 ± 0.039	1.030 ± 0.017	1.723 ± 0.043
0.092	0.185 ± 0.001	0.090 ± 0.005	1.284 ± 0.005	0.706 ± 0.027	1.328 ± 0.083	0.949 ± 0.012	1.881 ± 0.046
0.857	0.212 ± 0.010	0.121 ± 0.015	1.607 ± 0.039	0.752 ± 0.032	1.294 ± 0.045	0.969 ± 0.012	1.721 ± 0.013
0.094	0.203 ± 0.004	0.104 ± 0.013	1.309 ± 0.019	0.694 ± 0.026	1.318 ± 0.067	0.948 ± 0.002	1.899 ± 0.025
0.345	0.150 ± 0.023	0.101 ± 0.003	1.004 ± 0.011	0.697 ± 0.013	1.254 ± 0.050	0.921 ± 0.011	1.799 ± 0.038
0.416	0.234 ± 0.017	0.052 ± 0.004	0.653 ± 0.010	0.718 ± 0.019	1.160 ± 0.038	0.789 ± 0.010	1.616 ± 0.010
0.432	0.194 ± 0.001	0.052 ± 0.010	0.637 ± 0.013	0.726 ± 0.002	1.204 ± 0.019	0.830 ± 0.006	1.658 ± 0.022
0.663	–	–	0.880 ± 0.030	0.724 ± 0.017	1.202 ± 0.013	0.935 ± 0.003	1.660 ± 0.021
0.677	–	–	0.934 ± 0.031	0.689 ± 0.019	1.192 ± 0.007	0.967 ± 0.009	1.730 ± 0.038
0.687	–	–	0.836 ± 0.010	0.689 ± 0.021	1.176 ± 0.005	0.969 ± 0.015	1.707 ± 0.045
0.241	0.068 ± 0.005	0.031 ± 0.002	0.583 ± 0.002	0.688 ± 0.015	1.367 ± 0.018	0.921 ± 0.010	1.987 ± 0.017
0.276	–	–	0.576 ± 0.014	0.759 ± 0.019	1.330 ± 0.012	0.910 ± 0.002	1.752 ± 0.028
0.743	0.105 ± 0.004	0.072 ± 0.004	1.663 ± 0.005	0.716 ± 0.041	1.391 ± 0.037	0.990 ± 0.004	1.943 ± 0.060
0.780	0.087 ± 0.002	0.074 ± 0.006	1.715 ± 0.005	0.706 ± 0.026	1.349 ± 0.038	0.991 ± 0.028	1.911 ± 0.017
0.753	0.123 ± 0.008	0.092 ± 0.008	1.761 ± 0.036	0.726 ± 0.038	1.431 ± 0.021	1.011 ± 0.010	1.971 ± 0.074
0.794	–	–	1.760 ± 0.013	0.678 ± 0.031	1.426 ± 0.003	0.992 ± 0.023	2.103 ± 0.092
0.257	–	–	0.775 ± 0.016	0.710 ± 0.011	1.368 ± 0.030	0.933 ± 0.003	1.927 ± 0.012
0.294	–	–	0.850 ± 0.035	0.748 ± 0.016	1.370 ± 0.031	0.912 ± 0.020	1.832 ± 0.002

"–" No emission is detected.

cores of the Na I D_1, D_2 lines are weak filled-in absorption for the cooler component. In some cases, the Na I D_1, D_2 lines exhibit obvious excess emission from the cooler component.

The measured EWs of the excess emissions in the Na I D_1, line are plotted vs. the orbital phase in Fig. 4. For Na I D_1, it seems that there are two minima around the quadratures. That suggests an active longitude phenomenon during our observations.

The He I D_3 line is formed in the upper chromosphere and is an activity indicator for the Sun and late-type stars. The emission of the line is a probe for detecting flare-like events (Zirin 1988). In our set of 20 spectra in two different observing seasons, we observed no flare-like episodes.

4.2. The Ca II IRT lines

The Ca II IRT lines are important chromospheric activity indicators for the Sun and late-type stars (Shine & Linsky 1972; Shine & Linsky 1974; Linsky et al. 1979; Foing et al. 1989; Dempsey et al. 1993; Gunn & Doyle 1997; Montes et al. 1997, 2000; Andretta et al. 2005). They are formed in the lower chromosphere making them sensitive probes of the temperature minimum region (Montes et al. 1997).

For all the observed spectra (Fig. 1), we can see that the Ca II IRT absorption lines are from both components and that the cooler component shows strong filled-in absorption or sometimes even small self-reversal core emission. For the spectra during Nov. 28−30, 2006 and Dec. 8−10, 2006, we note that the Ca II 8498 line exhibits weak self-reversal emission in the line core, while the Ca II 8542 and 8662 lines show little or no such self-reversal core emission. For the spectra during Oct. 28, 29, 2006, especially the spectra on Oct. 28, 2006, all Ca II IRT lines exhibit obvious self-reversal in the line core. This is the strongest for the Ca II 8498 line, a little weaker for the Ca II 8542 line, and distinctly the weakest for the Ca II 8662 line.

The spectral subtraction reveals that the cooler component shows clear Ca II IRT excess emission. For the subtracted spectra, we measured the EWs of the excess emission and plotted vs. orbital phase in Fig. 4. From this figure, we find no significant
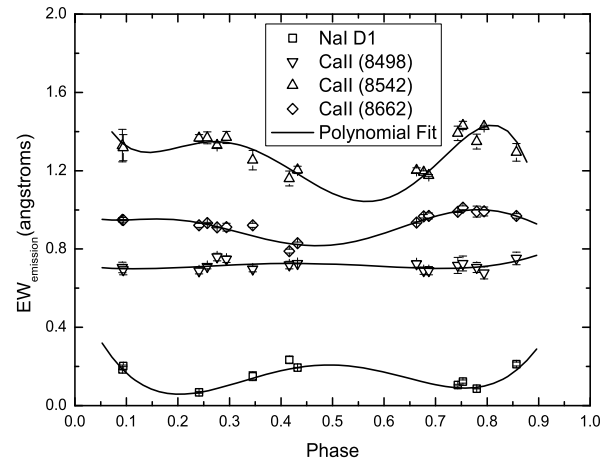
Fig. 4. The EWs of the excess emissions vs. orbital phase for Na I D and Ca II IRT lines. The solid line refers to a polynomial fit to the data.

trend in the Ca II 8498 data. For the Ca II 8542 and 8662 lines, especially for the Ca II 8542 line, it seems that there are two active longitudes near phases 0.25 and 0.75. In addition, the excess emission is also stronger (within the errors) at phase 0.09.

4.3. The H_α line

The H_α line is a very useful indicator of chromospheric activity, and it is formed in the middle chromosphere (Montes et al. 1997, etc.).

The H_α line exhibits variation from absorption to weak emission (see Fig. 1). Also, it is usually filled in with broad emission. All the subtracted H_α spectra indicate that the cooler component is active. Some excess emission profiles are broader and centered on the cooler component, for example, the spectra at phases 0.941 and 0.780. Furthermore, there are obvious absorption features in the subtracted spectra, at orbital phases 0.171, 0.424, 0.345, 0.663, 0.677, and 0.687. The EWs of the excess emissions for the 2006 data are plotted against orbital phase in
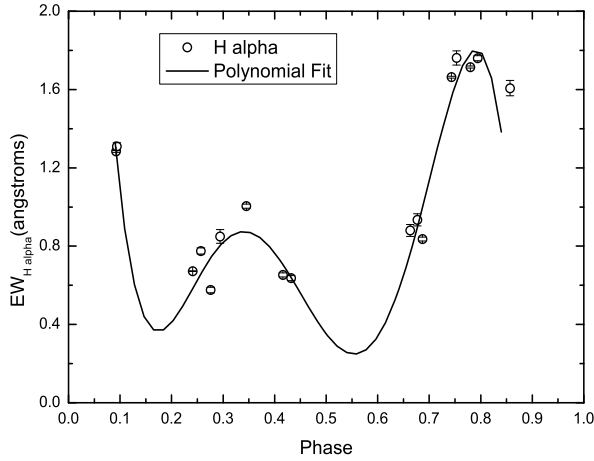
Fig. 5. As Fig. 4, but for the *EW*s of H_α line.

Fig. 5. The orbital modulation of the H_α excess emission is similar to Ca II 8542 and 8662 data. It seems that there are also two active longitudes near phases 0.35 and 0.75.

5. Discussion

In this paper, we analyze simultaneous spectroscopic observations of several optical chromospheric activity indicators for the RS CVn eclipsing binary system SZ Psc using the spectral subtraction technique. We investigate the details of the excess emission and study the chromospheric emission variation with orbital phase.

5.1. Chromospheric activity

For the Ca II IRT lines, we find the cooler component of SZ Psc shows filled-in absorption or sometimes even weak self-reversal core emission. This might be due to the low-level plage and high rotational velocity of the cooler component of SZ Psc. For some other chromospherically active binary systems, Montes et al. (2000) also detected a similar feature in the Ca II IRT lines.

For the most obvious self-reversal core emission feature, it is normal that the reversal is the strongest for the Ca II 8498 line, a little weaker for the Ca II 8542 line, and weakest of all for the Ca II 8662 line. This is consistent with the observation of the CaII IRT lines of solar plages with different degrees of activity (Shine & Linsky 1972; Shine 1973; Shine & Linsky 1974). The increase in self-reversal core emission in the Ca II IRT lines results from the higher temperatures and higher electron densities at a given line optical depth produced by the steeper temperature gradient (Shine & Linsky 1974).

For the ratio between EW_{8542} and EW_{8498}, we find the values are generally low, between $1-3$, which indicates optically thick emission in plage-like regions. In solar plage, the values of EW_{8542}/EW_{8498} are in the range $1.5-3$ (Chester 1991). These low values are also found in other chromospherically active binaries by other authors: Lázaro & Arévalo (1997); Arévalo & Lázaro (1999); Montes et al. (2000); and Gu et al. (2002).

All the H_α spectra indicate that the cooler component is active. In the subtracted spectra, the excess emission profiles exhibit broad wings. The broad emission feature coincides with the results derived by other authors: Huenemoerder & Ramsey (1984), Eaton & Henry (2007), etc. There are a couple of possible explanations for this. First, the broad component could be interpreted as arising from microflaring. Such broad

H_α components are also detected in some other chromospherically active stars (Hatzes 1995; Montes et al. 2000; etc). Second, it might be caused by instantaneous mass transfer from the cooler component to the hotter one (Bopp 1981). Because the cooler component is filling 82% of its Roche lobe (Lanza et al. 2001), it is very possible that the mass transfer can happen due to the strong chromospheric activity.

In summary, all the analyzed activity indicators show that the cooler component is active. This is consistent with the result that the Mg II h&k emission lines are mainly enhanced by the cooler component of the system (Doyle et al. 1994a,b; Kang et al. 2003). Moreover, for the Ca II H and K lines of SZ Psc derived by Fernáandez-Figueroa et al. (1986) and Fernáandez-Figueroa et al. (1994), there is obvious emission from the cooler component and no emission from the hotter one.

5.2. Chromospheric activity modulation

For the non-eclipsed configuration, the modulation of excess emission with phase indicates the appearance and disappearance of discrete active regions as the star is presenting different hemispheres to us.

For the cooler component, our result suggests the presence of an active longitude phenomenon during the 2006 epoch. To demonstrate the possible rotational modulation well, we used polynomial function to fit the EWs of Na I D_1, Ca II IRT, and H_α excess emission profiles, which are displayed in Figs. 4 and 5. For the CaII 8542 and 8662 and H_α lines, the excess emissions (with the orbital phase) may be correlated basically, especially around two quadratures. It seems that the emissions are stronger around two quadratures of the system (phases 0.25 and 0.75). However, for the Na I D_1 line, it seems that the emission is weaker around the two quadratures, so the Na I D_1 line may be anti-correlated with the Ca II 8542 and 8662 and the H_α lines. The reason might be that the Na I lines could be affected by the presence of active spot regions, because the reactions of neutral atoms in their ground states are very sensitive to the photospheric temperature structure (Barradoy Navascués et al. 2001). Moreover, there is some evidence that two variable active regions appear around longitudes $50°$ and $270°$ by analyzing a sequence of *V*-band light curves of SZ Psc (Lanza et al. 2001). In addition, both active longitudes were also suggested by Huenemoerder & Ramsey (1984).

For another chromospherically active binary UX Ari, the favorite active longitudes are also around two quadratures of the system based on the analysis of several chromospheric activity indicators He I D_3, Na I D_1, D_2, H_α, and CaII IRT lines (Gu 2005). These active longitude features have also been found using photometry on many other active RS CVn binary systems, such as EI Eri, σ Gem, HK Lac, and RT And (Olah Hall & Henry 1991; Henry et al. 1996; Berdyugina & Tuominen 1998; and Zhang & Gu 2007).

5.3. The absorption features in H_α line.

The interesting result from our high-resolution H_α subtracted spectra is the detection of absorption components at some orbital phases in our observations. The physical properties of the absorptions are listed in Table 3, which includes orbital phase, the radial velocity measured with respect to the cooler component's frame of rest, and the EW of the absorption. Similar peculiarities can be found in the differential spectra of Huenemoerder & Ramsey (1984).

Table 3. Observed properties of the absorption features identified by Gaussian fitting.

Phase	absorption	RV(km s^{-1})	EW(Å)	absorption	RV(km s^{-1})	EW(Å)
0.171	absorption1	−111	0.124 ± 0.012	absorption2	97	0.061 ± 0.003
0.424	absorption3	−57	0.322 ± 0.003			
0.345	absorption1	94	0.322 ± 0.003			
0.416	absorption1	−123	0.052 ± 0.007	absorption2	−49	0.069 ± 0.001
0.432	absorption1	−93	0.064 ± 0.005	absorption2	−29	0.056 ± 0.006
0.663	absorption3	118	0.080 ± 0.008			
0.677	absorption3	133	0.067 ± 0.005			
0.687	absorption3	153	0.064 ± 0.006			

"RV" is the radial velocity measured with respect to the cooler component's frame of rest. Negative velocities represent blueshifts.

The absorption features may be explained by the stellar prominence. Stellar prominence results in relative absorption while passing between the stellar disk and the observer, and then scatters photons arising in the chromosphere out of the line of sight. This phenomenon was first reported by Collier Cameron & Robinson (1989) for the rapidly rotating star AB Dor. Since then, stellar prominence has been observed as transient absorption (usually) or emission crossing the profiles of the Balmer lines, not only in single stars but also in binary systems (Hall & Ramsey 1994; Cameron et al. 2002).

If the numbered features in Fig. 3 arise from prominences (and are not simply due to less active stellar surface areas or the velocity separation of the components.), we calculate the distances of the prominences from the rotation axis of cooler component, using the simple model (Collier Cameron & Robinson 1989). During Oct. 28, 29, 2006, the distances of the prominences1, 2, and 3 (see Fig. 3) are 3.8 R, 2.5 R, and 2.9 $R \pm 0.5$ R (R is the radius of the cooler component), respectively. For the prominence3, if we let it go back to the phase 0.432, the velocity of prominence3 should be −144 ± 51 km s^{-1}. On the other hand, the velocity of the prominence1 detected at phase 0.432 is just inside the range. Thus, prominence1 and prominence3 might came from the same place. During the 2004 observing season, the velocities of the two absorptions are −111 km s^{-1} blueward and 97 km s^{-1} redward of the central velocity of the cooler component at phase 0.171, and the velocity of the absorption3 feature is about 57 km s^{-1} blueward of the cooler component at phase 0.424. If absorption1 and 3 have the same prominence, the distance of the prominence is 1.7 R. The EW of the absorption3 is larger than one of the absorption1. This indicates that the prominence absorption should be much more visible against the disk of the cooler component from the phase 0.171 to 0.424, due to the much greater projected area. For absorption2 at phase 0.171, if the distance of the promience2 is 2.7 R (the average value of the distances of our observed prominences), when moving to 0.424, the radial velocity should be about 185 km s^{-1} redward of the cooler component. It is just the critical point of the excess emission, and absorption2 should not be visible against the stellar disk at phase 0.424. This is consistent with our result that there is no absorption feature at the critical point of the redward excess emission at phase 0.424.

In the course of the spectral analysis, it was found that there are some absorption components around the primary profiles at some phases such as 0.663, 0.667, and 0.687. These absorptions may also be a mass transfer effect since the cooler component is very close to its Roche lobe and the mass transfer occurs more easily when considering the strong magnetic activity. These phenomena are also found in other RS CVn stars by other authors: Huenemoerder et al. (1989), Hall & Ramsey (1992), Gu et al. (2002).

Unfortunately, our data do not cover the H$_\beta$ line. We cannot tell whether this is optically thick or thin structure via the ratio $EW_{H_\alpha}/EW_{H_\beta}$ (Huenemoerder et al. 1989). It is impossible to define the nature of the absorption precisely at present.

6. Conclusions

The results from the analysis of our spectral data of SZ Psc can be summarized as follows.

1. The chromospheric activity indicators Na I D$_1$, D$_2$, Ca II IRT and H$_\alpha$ lines show that the cooler component is active in the system.
2. We find that the EW_{8542}/EW_{8498} is in the range 1−3, which indicates optically thick emission in plage-like regions.
3. For the Ca II 8542 and 8662 and the H$_\alpha$ lines in 2006, it seems that the excess emissions are stronger near the two quadratures of the system. They may be anti-correlated with the behavior of the Na I D$_1$ line. These suggest the presence of the active longitude phenomenon during our observations.
4. The absorption features are detected in the subtracted H$_\alpha$ lines, which could be explained by prominence-like extended material seen on the stellar disk or mass transfer from the cooler component to the hotter one.

References

Andretta, V., Doyle, J. G., & Byrne, P. B. 1997, A&A 322, 266
Andretta, V., Busà, I., Gomez, M. T., & Terranegra, L. 2005, A&A, 430, 669
Antonopoulou, E., Deliyannis, J., & Mitrou, C. K. 1995, Inf. Bull. Var. Stars, No. 4262
Arévalo, M. J., & Lázaro, C. 1999, AJ, 118, 1015
Barrado y Navascués, D., García Lopez, R. J., Severino, G., & Gomez, M. T. 2001, A&A, 371, 652
Barden, S. C. 1985, ApJ, 295, 162
Berdyugina, S. V., & Tuominen, I. 1998, A&A, 336, L25
Bopp, B. W. 1981, AJ, 86, 771
Bopp, B. W., & Talcott, J. C. 1978, AJ, 83, 1517
Catalano, S., Frisina, A., Rodono, M., & Scaltriti, F. 1978, Inf. Bull. Var. Stars, 1427
Chester, M. M. 1991, Ph.D. Thesis, Pennsylvania State Univ.
Collier Cameron, A., & Robinson, R. D. 1989, MNRAS, 236, 57
Collier Cameron, A., Jardine, M., & Donati, J.-F. 2002, in Stellar Coronae in the Chandra and XMM-Newton Era, ed. F. Favata, & J. J. Drake, ASP Conf. Ser., 277, 397

Dempsey, R. C., Bopp, B. W., Henry, G. W., & Hall, D. S. 1993, ApJS, 86, 293
Doyle, J. G., Mitrou, C. K., Mathioudakis, M., et al. 1994a, A&A, 291, 135
Doyle, J. G., Mitrou, C. K., Mathioudakis, M., & Antonopoulou, E. 1994b, A&A, 283, 522
Eaton, J. A. 1977, Inf. Bull. Var. Stars, No. 1297
Eaton, J. A., & Hall, D. S. 1979, ApJ, 227, 907
Eaton, J. A., & Henry, G. W. 2007, PASP, 119, 259
Eaton, J. A., Scaltriti, F., Cerruti-sola, M., et al. 1982, Ap&SS, 82, 289
Fernández-Figueroa, M. J., De Castro, E., Montesinos, B., et al. 1986, Adv. Space. Res., 6, 187
Fernández-Figueroa, M. J., Montes, D., De Castro, E., & Cornide, M. 1994, ApJS, 90, 433
Foing, B., Crivellari, L., Vladilo, G., Rebolo, R., & Beckman, J. 1989, A&AS, 80, 189
Frasca, A., & Catalano, S. 1994, A&A, 284, 883
Frasca, A., Marino, G., Catalano, S., & Marilli, E. 2000, A&A, 358, 1007
Gálvez, M. C., Montes, D., Fernández-Figueroa, M. J., De Castro, E., & Cornide, M. 2007, A&A, 472, 587
Gray, R. O., Napier, M. G., & Winkler, L. I. 2001, AJ, 121, 2148
Gu, S.-H. 2005, in Coronal and Stellar Mass Ejections, IAU Symp. Proc. 226, Held 13−17 September, Beijing, ed. K. Dere, J. Wang, & Y. Yan (Cambridge: Cambridge University Press), 501
Gu, S.-H., Tan, H.-S., Shan, H.-G., & Zhang, F.-H. 2002, A&A, 388, 889
Gunn, A. G., & Doyle, J. G. 1997, A&A, 318, 60
Gunn, A. G., Doyle, J. G., & Houdebine, E. R. 1997, A&A, 319, 211
Hall, D. S. 1976, in Multiple Periodic Variable Stars, ed. W. Fitch (Dordrecht: Reidel), 287
Hall, J. C., & Ramsey, L. W. 1992, AJ, 104, 1942
Hall, J. C., & Ramsey, L. W. 1994, AJ, 107, 1149

Hatzes, A. P. 1995, AJ, 109, 350
Henry, G. W., Eaton, J. A., Hamer, J., et al. 1996, ApJ, 462, 888
Huenemoerder, D. P., & Ramsey, L. W. 1984, AJ, 89, 549
Huenemoerder, D. P., Buzasi, D. L., & Ramsey, L. W. 1989, AJ, 98, 1398
Jakate, S. M., Bakos, G. A., Fernie, J. D., & Heard, J. F. 1976, AJ, 81, 250
Jensch, A. 1934, Astron. Nachr., 252, 393
Kang, Y. W., Lee, W.-B., Kim, H.-I., & Oh, K.-D. 2003, MNRAS, 344, 1227
Lanza, A., Rodonò, M., Mazzola, L., & Messina, S. 2001, A&A, 376, 1011
Lázaro, C., & Arévalo, M. J. 1997, AJ, 113, 2283
Linsky, J. L., Hunten, D., Glacken, D., & Kelch, W. 1979, ApJS, 41, 481
Montes, D., Fernández-Figueroa, M. J., De Castro, E., & Cornide, M. 1995, A&A, 294, 165
Montes, D., Fernández-Figueroa, M. J., De Castro, E., & Sanz-Forcada, J. 1997, A&AS, 125, 263
Montes, D., Fernández-Figueroa, M. J., De Castro, E., et al. 2000, A&AS, 146, 103
Popper, D. M. 1988, AJ, 96, 1040
Ramsey, L. W., & Nations, H. L. 1981, PASP, 93, 732
Shan, H. G., Liu, X. F., & Gu, S. H. 2006, NA, 11, 287
Shine, R. A. 1973, Ph.D. Thesis, University of Colorado
Shine, R. A., & Linsky, J. L. 1972, SP, 25, 357
Shine, R. A., & Linsky, J. L. 1974, SP, 39, 49
Strassmeier, K. G., Hall, D. S., Fekel, F. C., & Scheck, M. 1993, A&AS, 100, 173
Tunca, Z. 1984, Ap&SS, 105, 23
Weiler, E. J. 1978, MNRAS, 182, 77
Wright, J. T., Marcy, G. W., Butler, R. P., & Voght, S. S. 2004, ApJS, 152, 261
Zirin, H. 1988, in Astrophysics of the Sun (Cambridge University Press)
Zhang, L. Y., & Gu, S. H. 2007, A&A, 471, 219